Available online at www.sciencedirect.com
SCIENCE DIRECT®
Sedimentary Geology 157 (2003) 235–252
Sedimentary Geology
www.elsevier.com/locate/sedgeo

Origin of dolomites in the Cretaceous Maha Sarakham evaporites of the Khorat Plateau, northeast Thailand

Mohamed El Tabakh [a,*], Cherdsak Utha-Aroon [b], John K. Warren [c], B. Charlotte Schreiber [d]

[a] School of Earth and Environmental Science, Queens College, Flushing, Queens, NY 11367, USA
[b] Economic Geology Division, Department of Mineral Resources, Rama IV, Bangkok, Thailand
[c] Department of Petroleum Geoscience, University of Darussalam, Tungku Link, Bandar Seri Begawan, Brunei
[d] Department of Geology, Appalachian State University, 195 Rankin Science Building, Boone, NC 28608, USA

Received 14 February 2001; accepted 13 May 2002

Abstract

The Khorat Plateau of northeast Thailand and Laos was an area of widespread deposition of evaporites and siliciclastics (Maha Sarakham Formation) during the Cretaceous and three types of dolomites are associated with this formation: (1) limpid dolomite, (2) coarse, subhedral and euhedral dolomite, and (3) saddle dolomite. Limpid dolomite is present as isolated crystals in recrystallized, clear halite beds while the other two types are only present as authigenic clusters and individual large crystals within the widespread Basal Anhydrite Unit (BAU) (1.1 m), which defines the lowest member of the formation.The $\delta^{18}O_{PDB}$ isotopic values and the $^{87}Sr/^{86}Sr$ ratios of the limpid dolomite are within the range of Cretaceous seawater. Petrography and carbon and oxygen isotopes suggest that limpid dolomite was formed under shallow burial during times of freshening in a mostly marine-fed aggrading halite salina. Dolomite formation was possibly influenced by bacterial metabolism. The coarse crystalline and saddle dolomite types float within a matrix of coarse, recrystallized anhydrite in the Basal Anhydrite. The $\delta^{18}O$ isotopic values of the coarse, subhedral and euhedral dolomite types are more negative than the limpid dolomite, and the $^{87}Sr/^{86}Sr$ ratios are more radiogenic than typical marine dolomite of the Cretaceous. Saddle dolomite has even more negative $\delta^{18}O$ isotopic values than the coarse euhedral dolomite. The $^{87}Sr/^{86}Sr$ ratios of the saddle dolomite are also radiogenic.The isotopic and petrographic data indicate that the dolomites in the Basal Anhydrite Unit are late and authigenic but do not appear to replace a precursor carbonate. Rather, they appear to have precipitated within the deep burial environment along a 1–2-m-thick subsurface mixing interface between warm upwelling basinal brines and dense highly saline brines created by dissolving the underside of the overlying impervious halite bed. The upwelling basinal waters presumably rose through the underlying siliciclastics of the Khorat Group and then moved laterally along the base of the Maha Sarakham salt. The result of this inferred hydrologic process apparently is an accumulation of burial dolomite and recrystallized residual anhydrite in a petrographically complex unit that ultimately appear to be a solution residue, the Basal Anhydrite Unit.
© 2002 Elsevier Science B.V. All rights reserved.

Keywords: Khorat Plateau; Thailand; Dolomites; Evaporites

1. Introduction

The halite beds of the Cretaceous Maha Sarakham Formation in Thailand contain minor limpid dolomite;

* Corresponding author.
E-mail address: eltabakh@hotmail.com (M. El Tabakh).

0037-0738/02/$ - see front matter © 2002 Elsevier Science B.V. All rights reserved.
doi:10.1016/S0037-0738(02)00235-X

however, two forms of dolomite (coarse subhedral to euhedral and saddle dolomite) are predominant in its basal member. These two forms are found only in the Basal Anhydrite Unit (BAU), which averages 1.1 m in thickness and in the immediately underlying sandstones and is overlain by a thick halite formation. This unit is interpreted to be a basin-wide diagenetic unit possibly created during burial by differential dissolution of the underside of the salt (El Tabakh et al., 1998a; Warren, 1999).

The origin of dolomite is not simple, as it can form in a number of ways, such as a primary precipitate, a diagenetic replacement or a high temperature hydrothermal/metamorphic phase (e.g. Folk and Land, 1975; Shinn et al., 1965; Shukla and Baker, 1988; Machel, 2000; Mazzullo, 2000). Given the multiplicity of source waters and the ability of one form of dolomite to evolve into another as the surrounding pore fluids change, an interpretation that a particular dolomite is a late stage or burial dolomite is often equivocal. That is, burial dolomite precipitated from basinal fluids with no dolomite precursor is thought to give similar, if not identical, textural and isotopic characteristics to a burial dolomite that is replacing a preexisting dolomite (Land, 1983; Gregg and Sibley, 1984; Sibley and Gregg, 1987).

It now seems that some dolomitization events begin early in the depositional/diagenetic cycle and are subsequently overprinted or cannibalized during burial dolomitization (Ayalon and Longstaffe, 1995; Gao et al., 1990, 1992; Montañez, 1994; Smith and Dorobek, 1993; Wojcik et al., 1994). In evaporite basins, dolomites are commonly associated with limestone and siliciclastic successions (e.g. Peryt and Scholle, 1996; Morad et al., 1995) and in these cases, dolomite crystals are coarse and form during burial of the evaporitic successions. In most of these cases, dolomite is formed by dolomitization by replacement of original carbonate strata under the influence of meteoric waters. However, in the dolomites documented in this paper, the possibilities of surface and near surface waters influencing early stages of dolomite precipitation in the BAU are nullified as the dolomites precipitated within an anhydrite matrix, possibly filling pore spaces between anhydrite crystals, which only formed itself during burial diagenesis. What makes this study unique is that dolomite in the BAU grew in a matrix that formed diagenetically and without the presence of earlier carbonates. By studying the style and relative timing of dolomite development in the Basal Anhydrite, we characterize authigenic burial dolomites that formed during the late diagenesis of the evaporites.

2. Material and methods

The Department of Mineral Resources (DMR) of Thailand provided 240 cores that were sampled during a comprehensive program for exploration of potash deposits in the Khorat Plateau of northeast Thailand. Dolomite samples were studied using X-ray diffraction and by conventional thin section petrography. The length of cores obtained range from 50 to 1100 m. A total of 100 thin section samples were prepared from the halite and anhydrite layers, which host the studied dolomites. Scanning Electron Microscopy and back-scattered electron imaging were used to define textural relationships between minerals. Samples of limpid dolomite were picked from dissolved residues of halite samples and were examined by X-ray diffraction in order to define their mineralogy. Dolomite crystals in the Basal Anhydrite Unit were obtained from polished sample cuts by using 0.1-mm-diameter rotary drills. Powder dolomite samples were split for carbon and oxygen isotopic analysis and for $^{87}Sr/^{86}Sr$ isotopic ratios. Thirty-four dolomite samples were analyzed for $\delta^{18}O_{PDB}$ and $\delta^{13}C_{PDB}$ values by using the method originally outlined by Craig (1957). The $\delta^{18}O$ and $\delta^{13}C$ isotopes were obtained by a Vacuum Generator SIRA-9 and standard deviation for the NSB-20 standard was 0.07 $(n-4)$ for $\delta^{18}O$, and 0.05‰ and 0.05‰ for $\delta^{13}C$. Precision of measurement of the $\delta^{18}O$ and $\delta^{13}C$ of dolomite samples is 0.1‰. Details of the analytical procedure and methods used for the isotopic analysis of $^{87}Sr/^{86}Sr$ ratios are given in El Tabakh et al. (1998a). Samples were normalized to NSB SRM 987 + 0.71025 and standard error uncertainties were less than 0.00002.

3. Maha Sarakham Formation

The Cretaceous Maha Sarakham Formation is up to 1.1 km in thickness and was deposited in an extensive foreland basin setting called the ‘Khorat Plateau’, which is situated on the Indochina microplate in

Thailand and Laos of Southeast Asia (Fig. 1). The Khorat foreland basin fill is dominated by about 4-km-thick, nonmarine red beds of the Khorat Group and the plateau is presently bounded by a high escarpment of about 900 m above sea level along its western edge where thrusted sheets of Carboniferous and Permian carbonates are exposed. Thrusting of these Paleozoic limestones took place during latest Paleozoic and early Mesozoic (El Tabakh and Utha-Aroon, 1998 and references therein). The plateau is a part of the Indochina microplate and includes the Sakon Nakon and Khorat basins, which are separated by the Phu Phan suture zone. These basins resulted from late-stage tectonic relaxation or extension that created half-graben basins that took place during most of the Mesozoic Era, and eventually filled with nonmarine deposits of about 4 km thick. Deposits of the Khorat Group include arkose, conglomerate and shale accumulated in lacustrine, fluvial and alluvial environments and lack carbonate deposits.

The Maha Sarakham Formation (Fig. 2) is an extensive evaporite succession showing striking stratigraphic similarity throughout the Khorat Plateau in northeastern Thailand. The formation was sampled by 240 cores and all cores show consistent lithologic similarity in the formation. The formation is com-

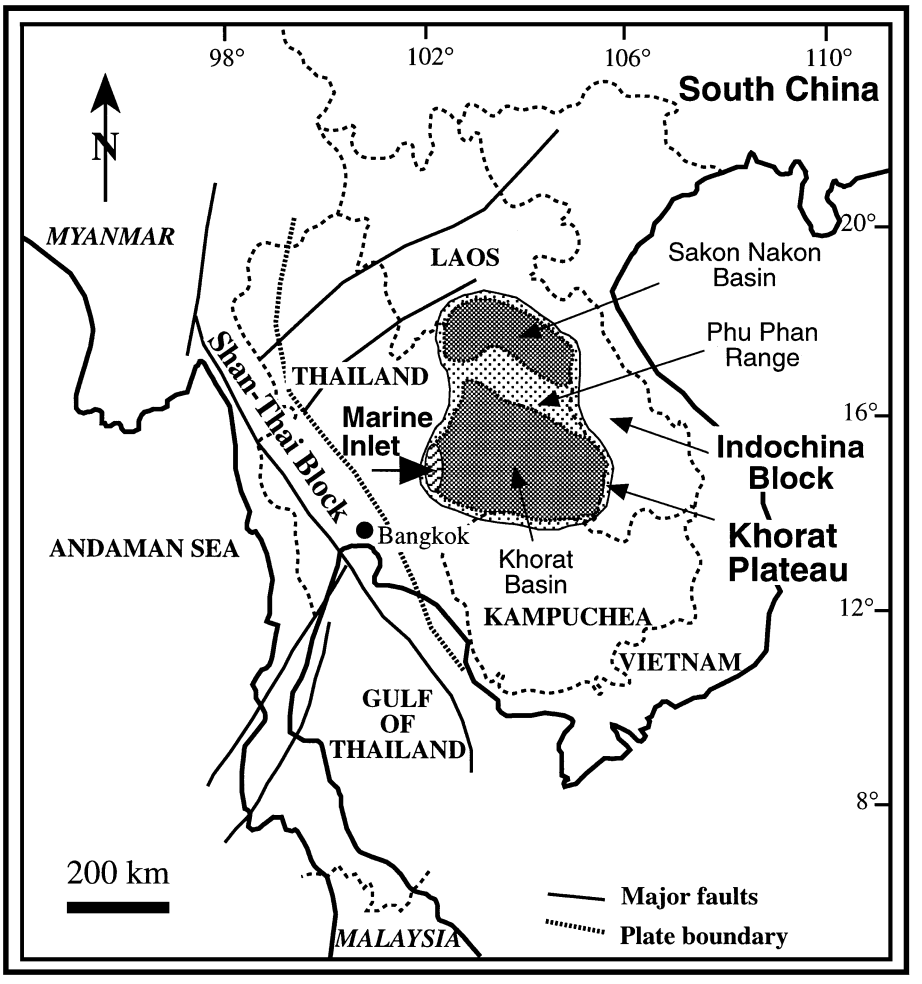

Fig. 1. Geological map of Southeast Asia showing the general tectonic elements of the region and the location of the Khorat and the Sakon Nakon basins in the Khorat Plateau area.

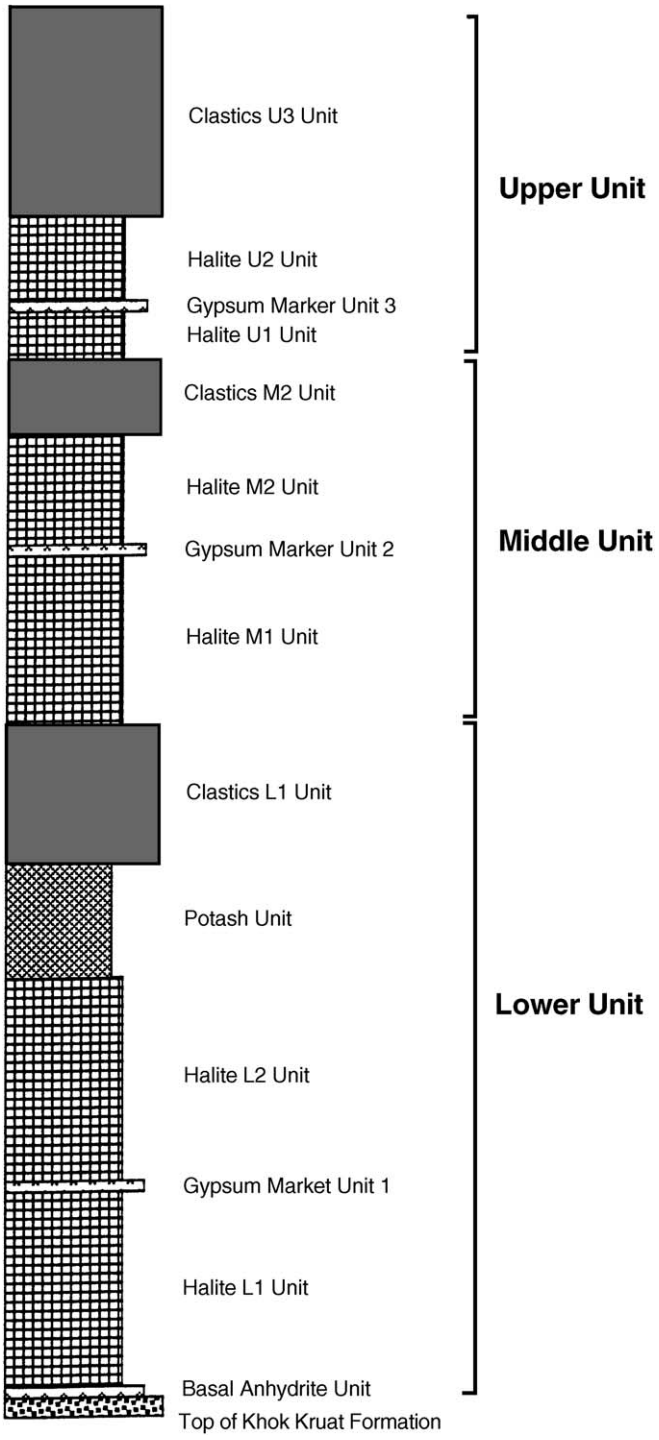

Fig. 2. Lithostratigraphy of a complete sedimentary section of the Cretaceous Maha Sarakham Formation showing three evaporative cycles interbedded with red-colored clastics. Complete description of sedimentary units is given in El Tabakh et al. (1998a,b).

posed of three members (lower, middle and upper). Each member includes halite and anhydrite deposits, interbedded with nonmarine red beds (Utha-Aroon, 1993; El Tabakh et al., 1998a,b). The formation averages 250 m in thickness increasing to 1.1 km thick in the center of the Khorat Basin where halokinesis has led to localized thickening and salt doming. The three distinctive members are composed of bedded evaporites of halite and anhydrite, separated by red siliciclastics. Clastics are fine-grained and are thick bedded with characteristic cross-bedding and lamination. Potash deposits of sylvite and carnallite are commonly present at the top of the lower halite member. The halite beds average 20 cm in thickness and are sporadically interbedded with thin, laminated anhydrite layers and halite-replaced pseudomorphs of bottom-growth gypsum, some 10–20 cm thick.

Halite layers are numerous, well bedded and have many halite crystals, and commonly retain chevron fabrics made up of aligned crystals ranging from 1 to 2 cm in size. Less common are clear, coarsely recrystallized halite bands (no chevrons) made up of interlocking crystals that average 5 cm across. It is adjacent to, or within these intrasalt calcium sulphate beds and some clear halite beds that the limpid dolomite occurs. The primary fabrics in halite beds are composed of chevron halite crystals, halite-replaced gypsum that are vertically oriented, and equant and recrystallized halite. These textures indicate shallow saline pan depositional environment. Sedimentary features and depositional fabrics such as cyclic deposition of halite and gypsum layers of the studied evaporites in all of the three units suggest recurrent flooding by shallow marine waters over the extensive area of the Khorat Plateau. Deposition of terrigenous layers became widespread during drying periods. These depositional features are akin to a marginal marine area adjacent to an isolated salt pan (El Tabakh et al., 1998a,b).

The Basal Anhydrite Unit (BAU) is found at the bottom of the Maha Sarakham Formation throughout both the Khorat and Sakon Nakhon basins with a consistent basin-wide thickness of 1.1 ± 0.3 m (El Tabakh et al., 1998a; Warren, 1999). Basin-wide drilling has shown the unit does not interfinger with, or pass laterally into, carbonates or clastics, and it is directly underlain by clastics of the Khok Kruat Formation, the uppermost formation of the Khorat Group (El Tabakh et al., 1998a). Internally, the anhydrite in the BAU exhibits laminar and stylolitized nodular forms. It has a sharp and stylolitic basal contact with the underlying sandstones of the Khok Kruat Formation (Fig. 2). Generally, the BAU is made up of poorly defined layers of hard, milky white to bluish-colored nodules. Anhydrite crystals show distorted and sheared mosaic fabrics (Fig. 3A). The BAU is characterized internally by repeated irregular stylolitic surfaces (Fig. 3B), which outline irregular nodular layers of anhydrite. Generally, this anhydrite is very coarse and exhibits elongated crystals up to 5 mm long (Fig. 3C). Along the stylolite surfaces, especially near the base of the BAU, there are occasional mm-sized clumps of metal sulfides, such as galena and pyrite.

El Tabakh et al. (1998a) interpreted the anhydrite in the Basal Anhydrite Unit to be a residual accumulation formed diagenetically via the leaching of halite along the underbelly of the lower halite member with the anhydrite accumulation as a residuum. Its near-constant thickness suggests an internal permeability-controlled feedback along the entire dissolution surface of the dissolving Maha Sarakham halite (El Tabakh et al., 1998a; Warren, 1999). The uniform formation of the BAU has most likely resulted from: (1) uniform deposition and widespread distribution of the overlying halite, (2) uniform and widespread underlying sandstones of the Khorat Group, (3) lack of tectonic structures such as faults or folds in the underlying sandstone layers, and (4) even basin-wide dissolution of the base of the salt.

4. Limpid dolomite

4.1. Petrography

Limpid dolomite comprises $\ll 1\%$ of the volume of any halite/sulphate unit. These dolomite crystals typically occur between clear halite crystals, just below a dm-thick bed of gypsum pseudomorphs or within layers of clear, recrystallized halite, which formed during flooding of the salt pan and formation of gypsum and anhydrite crystals. Individual dolomite crystals are clear, lack zonation, lack inclusions and may exhibit multi-crystal faces (Fig. 4A and B). The limpid dolomite is concentrated along boundaries of

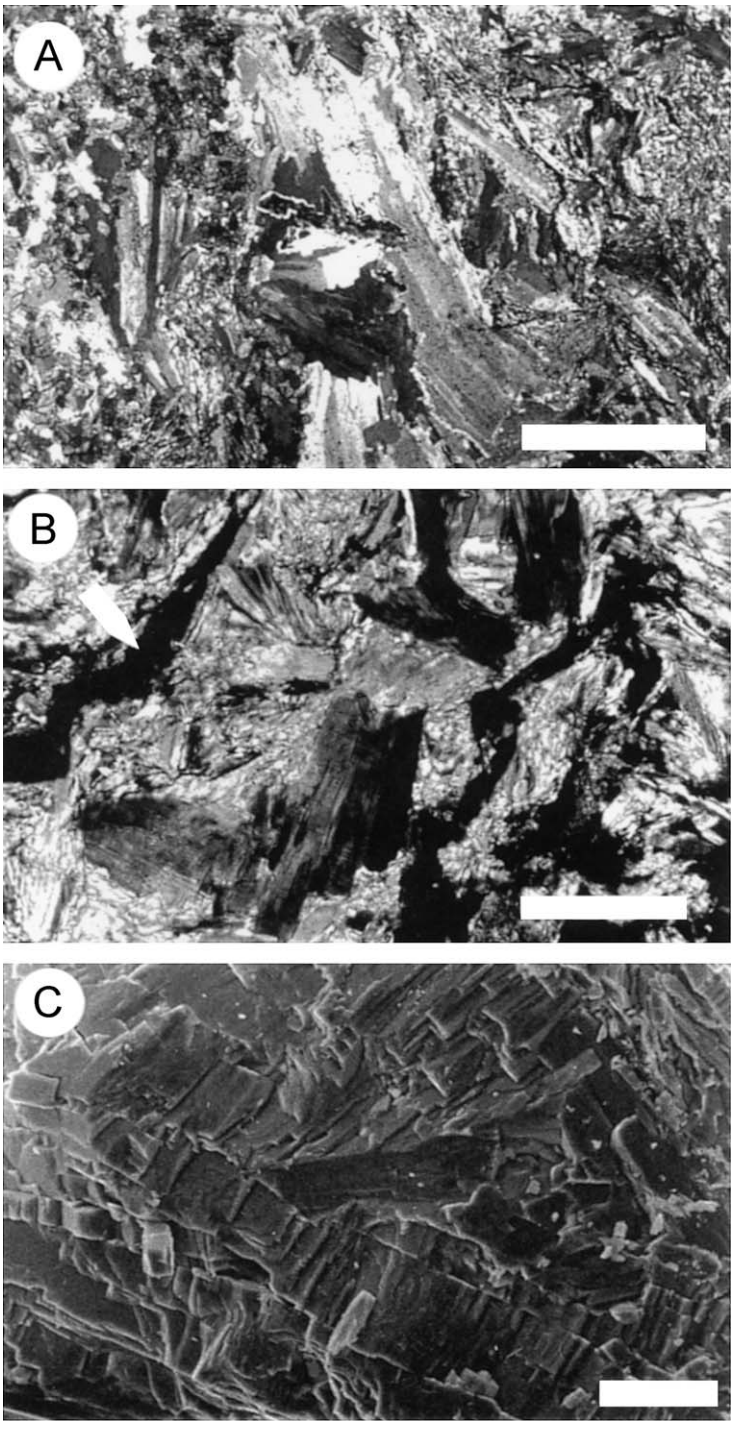
A
B
C

halite crystals or sutures either as individual or clusters of crystals that grew on halite crystal surfaces (Fig. 4C). The limpid dolomite crystals average 20 μm across and have diverse crystal shapes ranging from typical rhombs to polyhedral crystals. Most of the limpid dolomites in the Maha Sarakham tend to occur within intercrystalline pores within recrystallized halite immediately below an anhydrite marker bed.

4.2. Isotopes

Nine samples of halite from the lower halite member, taken from different cores located at different parts of the basin, were dissolved in distilled water and limpid dolomite crystals were then picked from washed and dried residues. X-ray diffraction showed the limpid dolomite is well ordered and near stoichiometric, as is the case with many evaporitic dolomites worldwide (Ali et al., 1993; Lloyd et al., 1985; Lumsden and Lloyd, 1997; Sperber et al., 1984). $\delta^{18}O_{PDB}$ isotopic values in the limpid dolomite range from −1.6‰ to −3‰, while $\delta^{13}C_{PDB}$ values range from +1‰ to −0.6‰ (Table 1). A cross-plot of $\delta^{18}O$ and $\delta^{13}C$ values (Fig. 5) shows that both the oxygen and carbon isotopic values are somewhat lighter than the average values of Cretaceous seawater (Veizer and Hoefs, 1976; Moss and Tucker, 1995: $\delta^{18}O$ ranges from −1.5‰ to −3.6‰ and $\delta^{13}C$ from +1.0‰ to +3.0‰. The $^{87}Sr/^{86}Sr$ ratios of the limpid dolomite range from 0.70712 to 0.70724; they are at the lower end of the Cretaceous seawater values, which range from 0.7071 to 0.7077 (Burke et al., 1982).

4.3. Discussion

The $\delta^{18}O$ and $\delta^{13}C$ values in the limpid dolomite are slightly lighter than early dolomites formed directly from Cretaceous seawater (e.g. marine values of Moss and Tucker, 1995). This suggests that the chemistry of any marine-derived brine seepage into the formative Maha Sarakham saline pan was modified before the limpid crystals formed. Their lighter values possibly reflect a combination of synsedimentary heating of the saltern brines, the influence of varying levels of meteoric input and the influence of bacterial metabolism on dolomite precipitation. Bacterially mediated dolomites with $\delta^{13}C$ of −2‰ to −9‰ are forming today in anoxic marine brines of the Lagoa Vermelha salina, Brazil (Vasconcelos, 1994; Vasconcelos and McKenzie, 1997), but their oxygen values are somewhat higher than those of the limpid dolomite. Likewise, the Sr isotope values in the limpid dolomite, which lie at the limit of typical Cretaceous marine values, which range from 0.7071 to 0.7077, support a modified rather than normal marine brine source. Using Mathews and Katz's (1977) equation, the temperature of crystallization suggests that the limpid dolomites formed at temperatures of 35 to 40 °C, which are typical temperatures of saline water bodies. Based on modern analogues, the temperature of surface and near water brines in the Maha Sarakham saline pans may be ranging between 25 and 45°C and may have occasionally reached 50 °C, so the formation of limpid dolomite to be a near surface, early diagenetic pore cement is reasonable.

4.4. Origin of limpid dolomite

Limpid dolomite was defined by early studies as well-developed and clear dolomite crystals in halite layers of Stewart (1952), Folk and Siedlecka (1974), Weaver (1976) and Naiman et al. (1983). It is also documented in dissolution residues of salt domes (Taylor, 1937) and more recently as 'urban' limpid dolomite on limestone surfaces of buildings (Rodriguez-Navarro et al., 1997). Layers of the clear host halite are present as repetitive beds within the salts of the Maha Sarakham Formation; they indicate synsedimentary dissolution during flooding of the halite-saturated saltern (El Tabakh et al., 1998b). Such clear layers appear to reflect the more commonplace, short-term flooding events in the saline pans, perhaps tied to intense desert rainstorms, which freshened the brine pool and modified the dissolved halite into coarser sparry forms. These depositional conditions are also documented in ancient halite deposits such as in the Williston Basin (Counter-

Fig. 3. Photomicrographs showing the petrology of the anhydrite in the Basal Anhydrite Unit (BAU). (A) Recrystallized anhydrite exhibiting typical anhydrite crystal laths. Scale bar is 1 mm. (B) Recrystallized anhydrite where crystals are in different orientations and are terminated against a stylolite surface (at arrow) at the upper left corner of the photograph. (C) An SEM image of the anhydrite showing the blocky nature of crystals and the orthorhombic cleavage of the crystals. Scale bar is 0.2 mm.

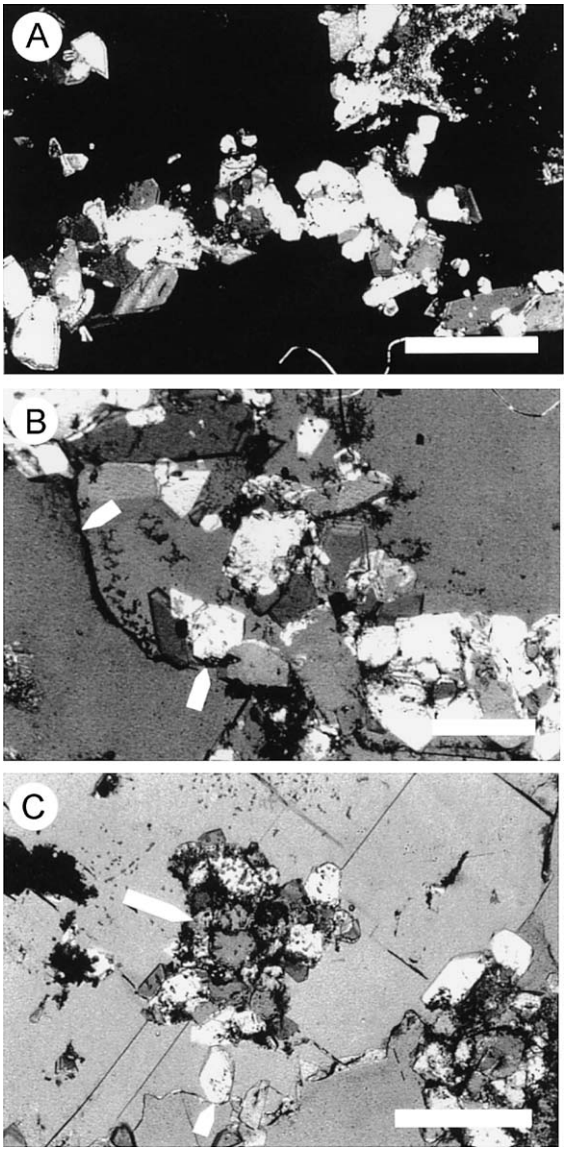

Fig. 4. Petrography of limpid dolomite found in clear halite layers. (A) Photomicrograph of a continuous string of limpid dolomite that grew on the edge of a clear halite crystal. Scale bar is 0.4 mm. (B) Photomicrograph of euhedral limpid dolomite crystals that mark the dissolution surface of a clear halite crystal (at arrows). Scale bar is 0.3 mm. (C) A photomicrograph of a cluster of limpid dolomite (arrow) found at the junction of equant and clear halite crystals. Scale bar is 0.4 mm.

Benison and Goldstein, 2000). There was little precipitation of gypsum re-corded in these sediments. Much of the bicarbonate, along with dissolved calcium and magnesium that formed the limpid dolomite in the clear halite units, was probably transported into the saltern in this mixed meteoric and evaporated water.

Occasional longer term floods or freshening (possibly marine-fed or related to regional climatic change) led to higher levels of calcium sulphate in the surface waters and the precipitation of dm- to m-thick gypsum layers (locally termed the "marker beds"). Gypsum crystals grew from atop dissolved and recrystallized halite substrate as layered and lenticular beds. With progressive evaporation after this longer term freshening, the saline pans eventually reattained long-term

Table 1
Isotopic values of the various Maha Sarakham evaporites

Dolomite type	$\delta^{18}O_{PDB}$	$\delta^{13}C_{PDB}$	$^{87}Sr/^{86}Sr$
Limpid dolomite	−1.6	−0.6	0.7071
Limpid dolomite	−1.9	+0.5	0.7071
Limpid dolomite	−2.1	+0.2	0.7072
Limpid dolomite	−2.2	−0.2	0.7071
Limpid dolomite	−2.6	+0.2	0.7072
Limpid dolomite	−2.8	−0.3	0.7072
Limpid dolomite	−2.9	+0.3	0.7071
Limpid dolomite	−2.9	−0.1	0.7072
Limpid dolomite	−3.0	+0.1	0.7072
Coarse dolomite	−3.8	+0.4	0.7073
Coarse dolomite	−6.2	+1.9	0.7073
Coarse dolomite	−4.4	−0.4	0.7074
Coarse dolomite	−4.6	−0.9	0.7073
Coarse dolomite	−4.5	−2.4	0.7074
Coarse dolomite	−5.2	+0.6	0.7073
Saddle dolomite	−8.2	−0.3	0.7073
Saddle dolomite	−9.5	+0.4	0.7073
Saddle dolomite	−10.0	−1.0	0.7074
Saddle dolomite	−10.2	−0.1	0.7073
Saddle dolomite	−10.6	−0.6	0.7074
Saddle dolomite	−10.8	−0.8	0.7073
Saddle dolomite	−10.8	−0.9	0.7074
Saddle dolomite	−10.9	−0.9	0.7073
Saddle dolomite	−10.8	+0.4	0.7073
Saddle dolomite	−11.0	+0.5	0.7074
Saddle dolomite	−11.2	+0.8	0.7075
Saddle dolomite	−11.4	+1.2	0.7075
Saddle dolomite	−11.8	+1.2	0.7074
Saddle dolomite	−11.9	−0.1	0.7075
Saddle dolomite	−12.3	−0.4	0.7074
Saddle dolomite	−13.8	−0.6	0.7075
Saddle dolomite	−14.0	−1.0	0.7076
Saddle dolomite	−14.3	−1.4	0.7076
Saddle dolomite	−14.4	−1.6	0.7075

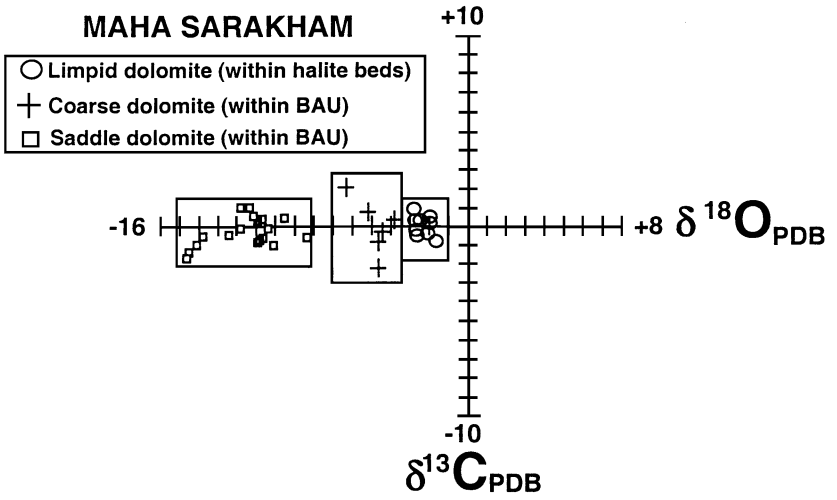

Fig. 5. Cross-plots of dolomite $\delta^{18}O$ and $\delta^{13}C$ isotopic values from the three types of dolomite found in the evaporites of the Maha Sarakham Formation.

halite saturation. However, as this occurred, the sinking halite saturated brines displaced the less dense sulphate pore brines resulting in the underlying gypsum being replaced/pseudomorphed by halite. This process also released Ca ions into the basin fluids (Hovorka, 1992; Schreiber and Walker, 1992). At the same time, the magnesium levels were high in the sinking liquors, reflecting the conservative chemical behavior of magnesium in NaCl brines. It was under these increasingly concentrated brine conditions following a longer term flooding event that mixing of fluids with different salinities precipitated most of the early diagenetic limpid dolomite. Such conditions are similar to those where dolomites form in sabkha environments (McKenzie et al., 1980) and the sulphate anions will not inhibit dolomite precipitation in hypersaline waters.

Several lines of evidence suggest that the limpid dolomite formed as early diagenetic mineral in the Maha Sarakham salt pan, including: (1) its widespread occurrence and presence at halite dissolution surfaces, (2) repeated evaporitic layers of halite indicate that limpid dolomite is much earlier and more widespread than in previously documented occurrences of freshening (e.g. Naiman et al., 1983; Gao et al., 1990), and (3) isotopic data of carbon, oxygen and strontium further support early diagenetic origin of the dolomite. Limpid dolomite early formation also reflects high concentration of magnesium in Cretaceous seawater (Stanley and Hardie, 1999).

5. Subhedral to euhedral dolomite

5.1. Petrography

Subhedral to euhedral crystalline dolomite only occurs in the Basal Anhydrite Unit, where it is abundant. The individual crystals of dolomite appear to be ‘floating’ within recrystallized anhydrite (Fig. 6). These crystals are pale brown in color and unimodal, some display cloudy centers and clear rims (Fig. 6A and B). They may reach up to 100 μm in size; however, the average crystal size is 70 μm. Crystals of coarse dolomite are concentrated along stylolite surfaces and construct aggregates along zones parallel and adjacent to the dark insoluble residues that outline the stylolites. Stylolites also separate layers of finer crystalline from coarser crystalline dolomite rhombs (Fig. 6B and C). Dolomite crystal size typically increases towards the stylolite zone. Increasing crystal size in the dolomites is parallel to increasing the size of the surrounding anhydrite. Larger dolomite crystals also exhibit curved crystal surfaces and splayed crystal orientations that define them as transitional forms into saddle dolomite described in the next section. The

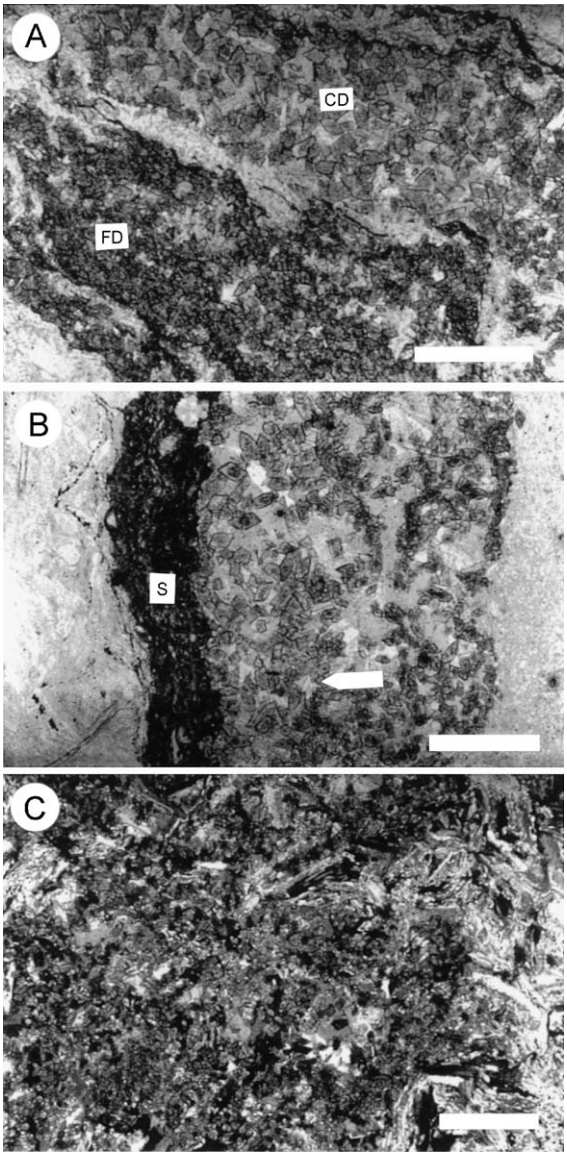

Fig. 6. Petrology of the coarse dolomite in the Basal Anhydrite Unit. (A) A photomicrograph showing two types of euhedral dolomite (CD: coarse dolomite and FD: fine dolomite) that are separated by a stylolite zone at the middle of the picture. Scale bar is 1 mm. (B) A photomicrograph showing dolomite crystal size increasing towards the stylolite surface. Arrow points toward the direction of increase of crystal size. Scale bar is 1 mm. (C) Coarse dolomite crystals within recrystallized anhydrite. Anhydrite crystals are of different orientation. Scale bar is 1 mm.

coarsest dolomite is commonly enclosed between large anhydrite crystals that are randomly oriented. X-ray diffraction analysis shows this coarse dolomite to be well ordered and near stoichiometric with 50% to 51% $CaCO_3$.

5.2. Isotopes

The $\delta^{18}O$ isotopic values of the six coarse dolomite samples range from -3.8‰ to -6.2‰ (Fig. 5). The $\delta^{13}C$ values range from $+1.9$‰ to -2.4‰. The $^{87}Sr/^{86}Sr$ ratios of these six dolomites are more radiogenic than typical marine carbonate of the Cretaceous age and range from 0.7073 to 0.7075 (Table 1).

5.3. Discussion

The coarse crystalline dolomites are found only in the Basal Anhydrite and are always in close association with stylolite surfaces. The well-ordered and near-stoichiometric nature of this dolomite suggests precipitation under relatively stable conditions, perhaps aided by dissolution–reprecipitation of earlier crystals. The relatively negative $\delta^{18}O$ values indicate crystallization at temperatures significantly above those of Cretaceous surface brines. The elevated $^{87}Sr/^{86}Sr$ ratios of the coarse dolomite indicate that the Sr is radiogenic and probably derived from pore fluids that had interacted with detrital feldspars and clays during burial. This strontium could have been driven from the underlying Khorat Group, which is a thick red bed sequence rich in feldspars. The extra magnesium needed to improve the dolomite stoichiometry was most likely derived from these basinal diagenetic waters as they interacted with the matrix of the aquifer or resulted from pressure dissolution of earlier dolomite.

6. Saddle dolomite

6.1. Petrography

Saddle dolomites in the Basal Anhydrite Unit are characterized by: (a) coarse crystals that average 1.5 mm, (b) subhedral to euhedral crystal shapes, (c) a lack of replacement textures or other evidence of any precursor carbonate, (d) abundant inclusions, (e) an association with stylolites and coarse, sparry and recrystallized anhydrite, and (f) euhedral crystals that

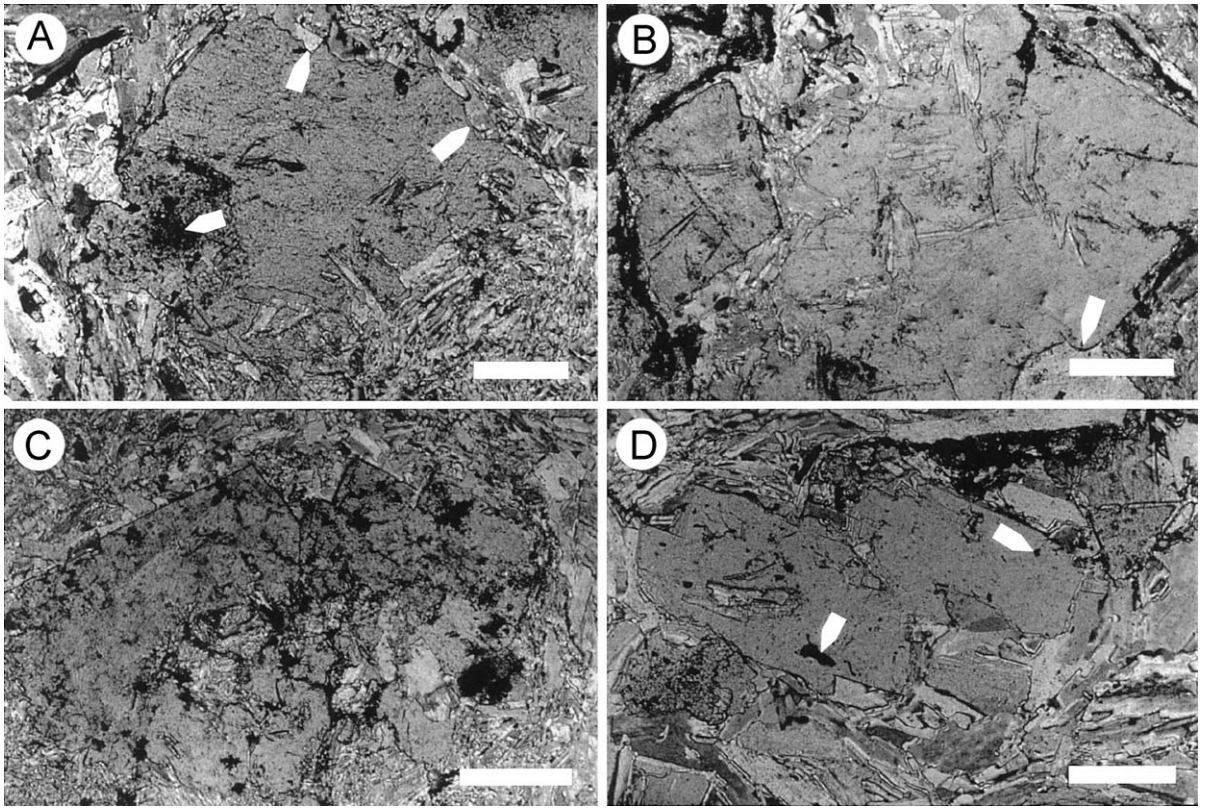

Fig. 7. Petrology of the saddle dolomite in the Basal Anhydrite Unit. (A) A photomicrograph of a subhedral dolomite crystal with numerous dark, fluid inclusions found within recrystallized anhydrite (arrow points to left) and irregular crystal rims (two other arrows). Scale bar is 0.5 mm. (B) Very coarse saddle dolomite crystal that almost fills the field of view with minor laths of anhydrite inclusions. Some of the crystal edges are curved (at arrow). Scale bar is 0.5 mm. (C) A group of subhedral dolomite crystals forming typical saddle-shape forms. The lower parts of the crystals are marked by stylolites. Scale bar is 0.5 mm. (D) A large, subhedral dolomite crystal found 'floating' in anhydrite mass. Arrows point to fluid inclusions. Scale bar is 0.5 mm.

are individual, free growth forms lacking sutured contacts (Fig. 7). They exhibit characteristic curved surfaces and weak sweeping extinction, and these petrographic features clearly separate them morphologically from the coarse, subhedral to euhedral dolomites. Generally, the saddle dolomite crystals are unimodal, with nonplanar textures and are nearly equant. Saddle dolomite is intimately associated with the most intensely recrystallized anhydrite. The latter is made up of large, poorly oriented, elongated laths of sparry and blocky crystals up to 5-mm size. The dolomite crystals are white, except where they contain inclusions (Fig. 7A). The larger saddle dolomite crystals have irregular crystal rims near the contact with the surrounding anhydrite and may contain inclusions of laths of anhydrite crystals, implying poikiliotopic growth (Fig. 7B). Some saddle dolomite crystals contain numerous small fluid inclusions (Fig. 7A and C). Locally, the dolomite crystals show subhedral shapes and irregular crystal edges (Fig. 7D) that define stylolitic zones (Fig. 7B and C). Similar large and euhedral saddle dolomite crystals are also present as intergranular cements and overgrowths on sandstone grains in the uppermost section of the underlying Khok Kruat Formation (Fig. 8A and B).

6.2. Isotopes

The saddle dolomite crystals have $\delta^{18}O$ values that range from −8.2 ‰ to −14.2 ‰ and $\delta^{13}C$ values that range from +1.8 ‰ to −1.9 ‰ (Table 1; Fig. 4). Like

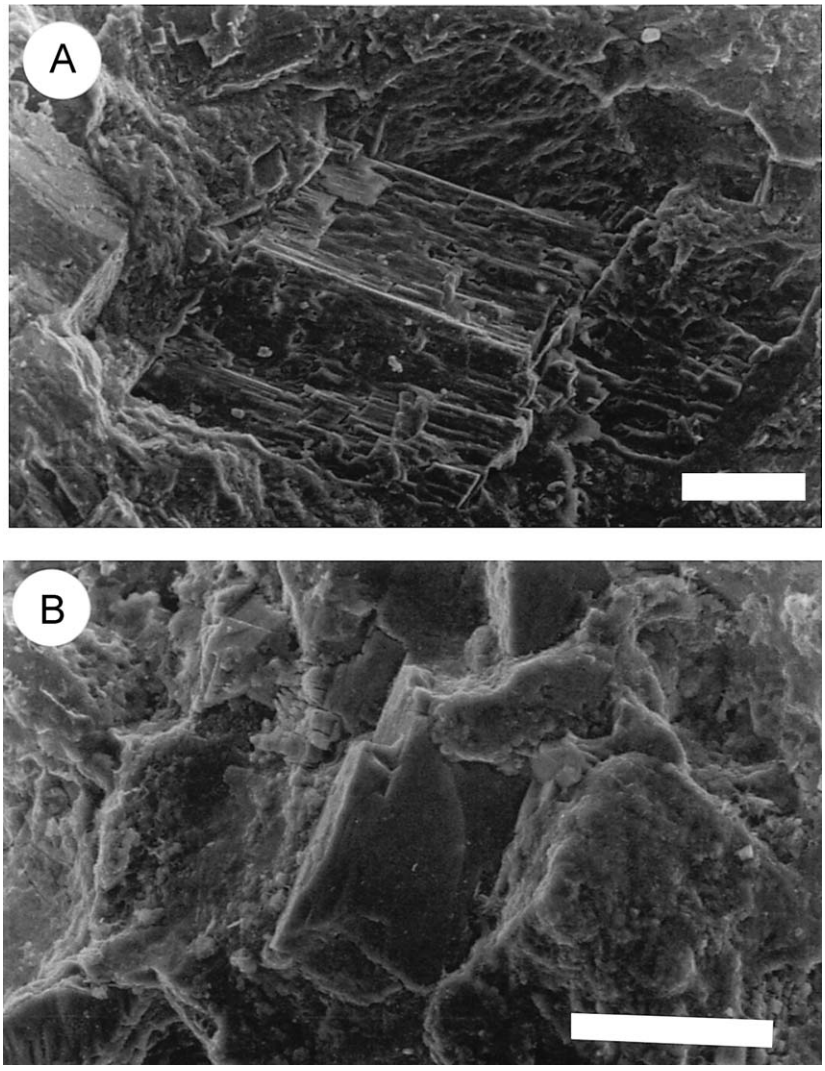

Fig. 8. SEM photomicrographs of dolomite crystals found in the sandstones of the Khuk Kruat Formation that lies just below the BAU. (A) Dolomite crystal with well-defined crystal boundaries showing intercrystalline porosity. Crystal is about 2 mm in size. Scale bar is 0.5 mm. (B) Dolomite crystal in center occurs between sand grains. Scale bar is 0.5 mm.

the coarse dolomite, the $^{87}Sr/^{86}Sr$ ratios of the saddle dolomites range from 0.70730 to 0.7076 and are radiogenic compared to Cretaceous-age, marine dolomite.

6.3. Discussion

Saddle dolomite is a burial mineral common in carbonate platforms worldwide (e.g. Zeeh et al., 1995; Vahrenkamp and Swart, 1994; Al-aasm et al., 2000) and those in the BAU are petrographically similar to those described by Radke and Mathis (1980), Krebs and Macqueen (1984), Lee and Friedman (1987) and Machel (1987). Saddle dolomite crystals have more negative $\delta^{18}O$ values than the other dolomites in the Basal Anhydrite or the Maha Sarakham. This suggests that saddle dolomite precipitation took place in hotter basinal waters compared with waters that precipitated the coarse and subhedral dolomite (described in the preceding section). The saddle dolomites exhibit the

most radiogenic and broadest values in Sr isotope ratios, which indicate once more a radiogenic source of the Sr in the pore water. This Sr was most likely obtained via pore–fluid interaction with the underlying siliciclastic rock matrix.

6.4. Origin of dolomite in the BAU

Potential sources of magnesium ions needed for dolomite formation are: (1) dissolution of evaporites, releasing magnesium ions into the pore waters; (2) dissolution/recrystallization of earlier dolomite (i.e. limpid dolomite); and (3) clay authigenesis in the underlying Khorat Group. Three possible origins are postulated for the formation of coarse and saddle dolomites in the Basal Anhydrite:

1) primary/penecontemporaneous precipitation during evaporative concentration/freshening,
2) recrystallization of a synsedimentary or early diagenetic dolomite or other early carbonate phase and,
3) authigenic and non-replacive precipitation of the coarse and saddle dolomites.

Petrographic analysis and isotopic data outlined in this paper constrain the origin and timing of formation of the coarse and saddle dolomites in the BAU; they support an authigenic, nonreplacement origin of coarse and saddle dolomites (possibility number (3) above) because of the following reasons.

(1) Forms of coarse and saddle dolomites are only found within the BAU and neither occur within the clear halite nor the anhydrite marker beds.

(2) The dolomite is found in close association with stylolites and compaction features in the BAU, which clearly supports formation in the burial environment.

(3) Dolomite crystals are typically pure, subhedral to euhedral forms, they lack calcite or salt inclusions or limpid cores, suggesting an authigenic origin from pore waters.

(4) The increase of dolomite crystal size towards stylolite surfaces provides direct evidence for pressure solution occurring during dolomite formation, when the stylolite surfaces were sites of active fluid throughput in the BAU.

(5) Coarsely crystalline and saddle dolomite is systematically associated with progressively coarser and recrystallized anhydrite, a diagenetic sulphate feature consistent with burial alteration. The presence of coarse dolomite with smaller anhydrite crystals relative to the saddle dolomite, which is always associated with sparry and larger crystallized anhydrite laths, is an important observation. This observation is consistent with progressive and intense diagenetic reactions of brines with evolving anhydrite crystals from fine to coarse crystalline.

(6) The Sr ratios in the coarse and saddle dolomites in the BAU indicate that diagenetic basinal fluids interacted with clastics of the underlying Khorat Group rocks, releasing radiogenic strontium.

(7) The negative oxygen isotopes in the coarse and saddle dolomites support precipitation in zones flushed by warm-to-hot basinal fluids.

Temperatures calculated from oxygen isotopes using Mathews and Katz's (1977) equation point to crystallization of the coarse, subhedral dolomite under temperatures of 45 to 60 °C, whereas the saddle dolomite formed under higher temperatures that ranged from 72 to 123 °C. The $\delta^{18}O$ values are also lower than those noted in Cretaceous dolomites elsewhere (Moss and Tucker, 1995). In contrast, the wide range of temperatures of crystallization shown by coarse and saddle dolomites in the BAU suggest interaction with hotter basinal fluids (Land and Lynch, 1996). Our petrographic observations and isotopic data show that the coarse subhedral dolomite and saddle dolomites within the Basal Anhydrite Unit were formed during burial diagenesis. The data given in the cross-plot of $\delta^{18}O$ values in dolomite versus $^{87}Sr/^{86}Sr$ ratios of the different types of dolomite (Fig. 9) in the Maha Sarakham Formation indicate that both types of dolomite have a distinctive and warmer isotopic provenance than the limpid dolomites in the halite. Pyrite and galena metals associated with dolomite in the BAU most likely resulted in pore fluids in part derived from transformation of smectite clays into illite in the burial environment (Dunoyer De Segonsac, 1970; Kaufman et al., 1990).

7. Why does dolomite precipitate at the base of the Maha Sarakham Formation?

During burial and compaction of the underlying Khorat siliciclastics, upwelling diagenetic fluids re-

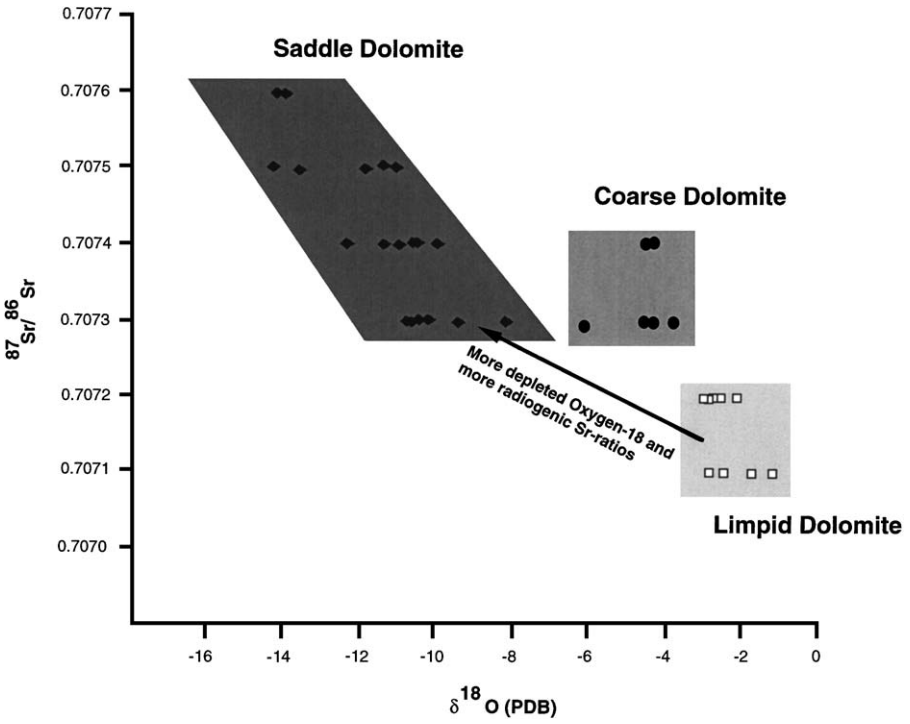

Fig. 9. A cross-plot of dolomite $\delta^{18}O$ values versus $^{87}Sr/^{86}Sr$ ratios and data indicate that the types of dolomite have distinctive isotopic signatures.

leased were Ca–Na–Cl–HCO_3 brines. Near the base of the Maha Sarakham salt, these basinal fluids mixed with more concentrated Ca–Na–Cl brines derived from halite dissolution. This mixing interface in evaporite basins worldwide is defined as a dynamic setting where many authigenic components are precipitated. In carbonate platform settings, however, mixtures of evaporative brines with freshwater have been reported as causes for dolomitization of carbonates deposited in restricted and evaporative environments (Machel and Mountjoy, 1986; Meyers et al., 1997). In these carbonates, saddle dolomite is commonly linked to late diagenetic fluids that are saline and hot (e.g. Coniglio et al., 1994; Drivet and Mountjoy, 1997; Lumsden and Lloyd, 1997; Yoo et al., 2000).

The Basal Anhydrite Unit is underlain by thick sandstone sequences of the Khorat Group and bound to the west by thrusts of exposed Permian carbonates (El Tabakh and Utha-Aroon, 1998). We are using the architecture of the Khorat Basin in order to suggest possible mechanisms responsible for supplying diagenetic fluids to the base of the Maha Sarakham Formation, and leading to the complex diagenetic reaction of the anhydrite, dolomite and salt.

These two possible mechanisms are: (1) extrabasinal topographic-driven recharge and (2) intrabasinal compactional due to sedimentary loading of salt and siliciclastics and convective fluid flow. The schematic model (Fig. 10) shows the proposed diagenetic system at the base of the evaporites, whereby both the coarse and saddle dolomites were precipitated as authigenic minerals within the BAU, as its anhydrite host was accreting and evolving via the dissolution of the underside of the Maha Sarakham salt. The same fluid/permeability feedback system that controlled the development of a uniform thickness of the BAU also facilitated the solution throughput that allowed the two types of burial dolomite to precipitate. This diagenetic process is similar to that of the evaporites and is associated with burial, compaction and stylolite formation and dolomitization in carbonate rocks.

Oxygen isotopic data for dolomites in the Basal Anhydrite show consistently negative values which

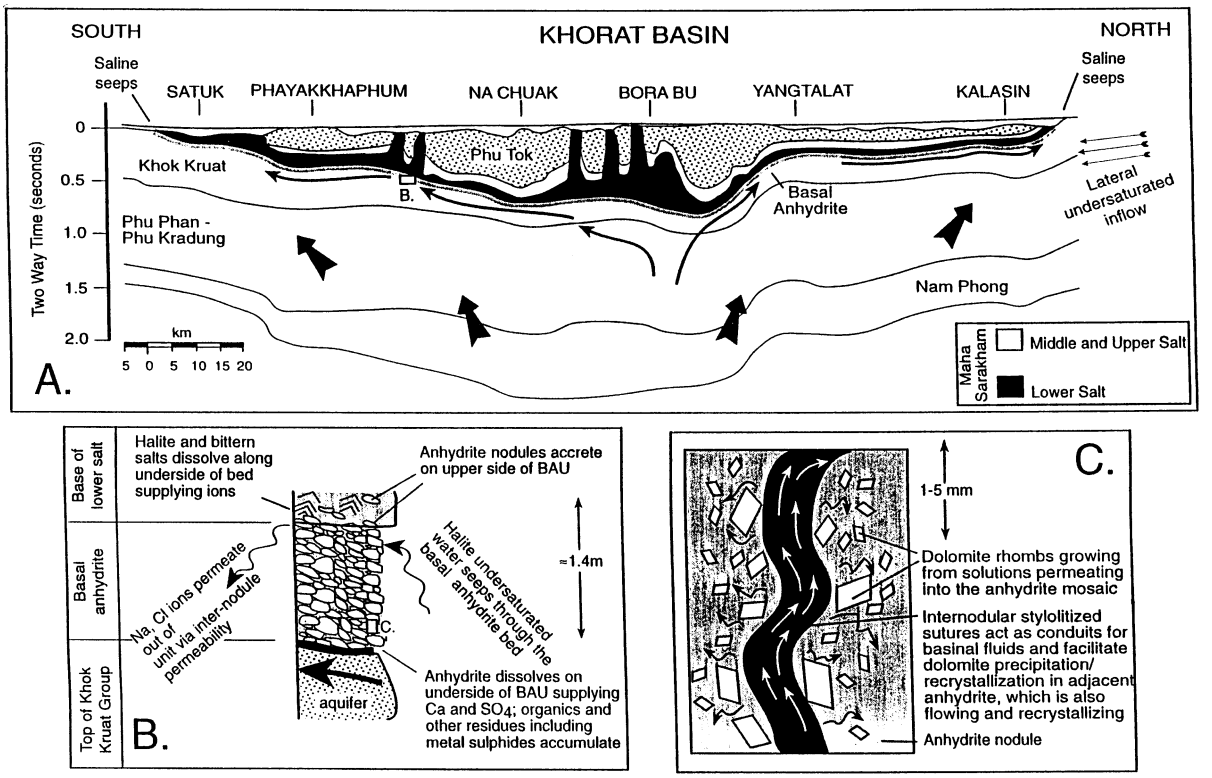

Fig. 10. A schematic model showing the proposed diagenetic system at the base of the Maha Sarakham Formation. (A) Convecting (density and thermal drive) basinal waters, along with compactional waters, circulate through a 5-km-thick sequence of nonmarine and feldspathic red beds that underlies the Maha Sarakham evaporites. The Basal Anhydrite forms in the zone of contact between upwelling cells of these basinal waters and the dissolving underbelly of the evaporites. (B) The basal contact of the Maha Sarakham evaporite sequence is a site of fluid flushing from below. It is characterized by dissolution and recrystallization where anhydrite is progressively recrystallized into coarse and sparry anhydrite. (C) Dolomite is precipitated, recrystallized and isotopically modified into various coarse and saddle dolomites adjacent to active stylolite sutures (black area in the middle). The stylolite suture facilitates the passage of the brines that carry the ions precipitated as the coarse and saddle dolomites. Hence, the decrease in rhomb size is away from the stylolite conduit.

reflect the influence of warm-to-hot subsurface waters that must have flowed through the Khorat siliciclastics. The permeability of the sandstones of the underlying Khok Kruat Formation is still partially retained and averages 20 md and the formation still acts as a low-conductivity aquifer. Sedimentary compaction, perhaps combined with topographic recharge, controlled the water flow pattern within the siliciclastics and caused either convection or simple upward flow of basin fluids. From the onset of their burial, basinal fluids have flushed and dissolved the base of the salt with the anhydrite accumulating as a residue. Deeply circulating basinal water moved upward by convection through the sandstone layers of the Khorat Group. However, once halite dissolution was initiated, brine plumes or density-driven convection would drive the system (Hanor, 1987) and it will continue until permeability is lost in the underlying sands, the halite is completely dissolved. Under these diagenetic conditions, including the dissolution of halite and of some of the anhydrite, stylolite seams were also forming where solubility contrast occurred between halite and anhydrite and facilitated stylolite formation.

The association of coarse dolomite with smaller anhydrite crystals, relative to the saddle dolomite with its sparry and largely recrystallized anhydrite host, is consistent with progressive and diagenetic reaction of basinal brines with the original anhydrite.

The schematic model (Fig. 10) shows the proposed diagenetic system at the base of the Maha Sarakham Formation. The stylolites were the fluid access pathways that facilitated dissolution and develop because of lithologic heterogeneities (Andrews and Railsback, 1997), and as shown in the next section, focused the formation of two types of burial dolomite. The notion that "active" stylolites act as fluid conduits in overpressured conditions has been documented in carbonates by Braithwaite (1986) and is also discussed in geopressured subsalt settings by Warren (1999) and in Iranian evaporites by Sadooni (1995).

That the siliciclastics of the Khorat Group were an important source of the dolomite-precipitating fluids at the base of the Maha Sarakham evaporites is confirmed by: (1) burial dolomites are concentrated along the contact between the halite and the siliciclastics, (2) the burial dolomites have slightly lighter $\delta^{13}C$ values than the limpid dolomite, (3) radiogenic ratios of Sr of dolomites in the BAU relative to those of the limpid dolomites indicate interaction of pore waters with siliciclastics. The association of these dolomites with stylolites also suggests formation during burial and compaction.

In most burial situations, a basinal aquifer carries hot brines that will facilitate re-equilibration of the early dolomite rhombs into coarse and saddle dolomites. In the case of the BAU, the evaporite has yet to be completely dissolved and so the overprint of the limpid rhombs by later diagenesis has yet to occur. It is a unique window in the realm of dolomite diagenesis not complicated by the presence of earlier platform carbonates. Burial dolomites are clearly evident here because the anhydrite matrix in which they grew appears to be a burial diagenetic unit that developed over the extensive region of the Khorat Plateau of Southeast Asia.

8. Conclusions

Petrographic and isotopic observations indicate that there are three types of dolomite in the Maha Sarakham evaporites including: (1) limpid dolomite present only in clear, virtually unaltered halite beds within the Maha Sarakham Formation, (2) coarsely crystalline dolomite in the BAU, and (3) saddle dolomite in the BAU. Additionally, galena and pyrite are also present along stylolite surfaces in the Basal Anhydrite Unit.

Limpid dolomite was formed as an authigenic mineral (non-replacive) in halite beds and nucleated on dissolution surfaces of halite crystals and along halite crystal sutures. This type of dolomite crystallized via mixing of dense halite-saturated brines. Textures in the halite host suggest that brine freshening was involved in the formation of the early diagenetic limpid dolomite.

Coarse subhedral and saddle dolomite types are present only in the BAU at the base of the Maha Sarakham Formation. These dolomites are associated with stylolites; dolomite crystal size increases towards the stylolitized zone. They represent burial dolomites interpreted to have precipitated from a basin-wide upwelling of warm-to-hot basinal waters with the dissolving base of the Maha Sarakham halite. Both the coarse and saddle dolomite crystals float within a recrystallized and stylolitized mass of burial anhydrite. Their $\delta^{18}O$ isotopic values attest to hot fluid involvement during formation of dolomite, while their $\delta^{13}C$ values attest to a contribution from organic-derived CO_2. The $^{87}Sr/^{86}Sr$ ratios of both burial dolomites are radiogenic, suggesting a basinal source of brine that experienced extensive rock/fluid interaction with feldspathic sandstones on its way through the underlying Khorat Group sediments.

Acknowledgements

The senior author acknowledges funding by a grant from the Australian Research Council (ARC). The staff of Department of Mineral Resources (DMR) of Thailand is thanked for their generosity in permitting this study of dolomite in the Khorat evaporites and for their field support. JKW would also like to acknowledge the ongoing support of the University of Brunei Darussalam for his research in Thailand. Reviews by Gregg Sibley, Eric Mountjoy and Bruce Sellwood greatly improved this paper.

References

Al-aasm, I., Ionnee, J., Clarke, J., 2000. Multiple fluid flow events and the formation of saddle dolomite: examples from middle Devonian carbonates of the western Canadian Basin. J. Geochem. Explor. 69–70, 11–15.

Ali, A.E., Barbin, V., Calas, G., Cervelle, B., Ramseyer, K., Bouroulec, J., 1993. Mn^{2+}-activated luminescence in dolomite, calcite, and magnesite: quantitative determination of manganese and site distribution by EPR and CL spectrospopy. Chem. Geol. 104, 189–202.

Andrews, L.M., Railsback, L.B., 1997. Controls on stylolite development: morphologies, lithologic, and temporal evidence from bedding-parallel and transverse stylolites from the U.S. Appalachian. J. Geol. 105, 59–73.

Ayalon, A., Longstaffe, F.J., 1995. Stable isotope evidence for the origin of diagenetic carbonate minerals from the Lower Jurassic Inmar Formation, southern Israel. Sedimentology 42, 147–160.

Braithwaite, C.J.R., 1986. Mechanically induced stylolites and loss of porosity in dolomites. J. Petrol. Geol. 9, 343–348.

Burke, W.H., Denison, R.E., Hetherington, E.A., Koepnick, R.B., Nelson, H.F., Otto, J.B., 1982. Variation of seawater $^{87}Sr/^{86}S$ throughout Phanerozoic time. Geology 10, 516–519.

Coniglio, M., Shrlock, R., Williams-Jones, A.E., Middleton, K., Frap, S.K., 1994. Burial and hydrothermal diagenesis of Ordovician carbonates from the Michigan Basin, Ontario, Canada. In: Purser, B.H., Tucker, M.E., Zenger, D.H. (Eds.), Dolomites: A Volume in Honour of Dolomieu. International Association of Sedimentologists, Special Publication, vol. 21, pp. 231–254.

Counter-Benison, K., Goldstein, R.H., 2000. Sedimentology of ancient salt pans: an example from the Permian Opeche Shale, Williston Basin, North Dakota, U.S.A. J. Sediment. Res. 70, 159–169.

Craig, H., 1957. Isotopic standards for carbon and oxygen correction factors for mass spectrometric analysis of carbon dioxide. Geochim. Cosmochim. Acta 12, 133–149.

Drivet, E., Mountjoy, E., 1997. Dolomitization of the Leduc Formation (Upper Devonian), southern Rimbey–Meadowbrook reef trend, Alberta. J. Sediment. Res. 67, 411–423.

Dunoyer De Segonsac, G., 1970. The transformation of clay minerals during diagenesis and low-grade metamorphism: a review. Sedimentology 15, 281–345.

El Tabakh, M., Utha-Aroon, C., 1998. Evolution of a Permian carbonate platform to siliciclastic basin: Indochina Plate, Thailand. Sedimentology 45, 579–594.

El Tabakh, M., Schreiber, B.C., Coshell, L., Utha-Aroon, C., Warren, J.K., 1998a. Diagenetic origin of basal anhydrite in the Cretaceous Maha Sarakham salt: Khorat Plateau, NE Thailand. Sedimentology 45, 579–594.

El Tabakh, M., Utha-Aroon, C., Schreiber, B.C., 1998b. Sedimentology of the Cretaceous Maha Sarakham evaporites in the Khorat Plateau of northeastern Thailand. Sediment. Geol. 123, 31–62.

Folk, R.L., Land, L., 1975. Mg/Ca ratio and salinity: two controls over crystallization of dolomite. Bull. Am. Assoc. Pet. Geol. 59, 60–68.

Folk, R.L., Siedlecka, A., 1974. The schizohaline environment: its sedimentary and diagenetic fabrics as exemplified by the Late Paleozoic rocks of Bear Island, Svalbard. Sediment. Geol. 15, 1015.

Gao, G., Hovorka, S.D., Posey, H.H., 1990. Limpid dolomite in Permian San Andreas halite rocks, Polo Duro Basin, Texas Panhandle: characteristics, possible origin, and implications for brine evolution. J. Sediment. Petrol. 60, 118–124.

Gao, G., Land, L.S., Folk, R.L., 1992. Meteoric modification of early dolomite and late dolomitization by basinal fluids, upper Arbuckle Group, Slick Hills, Southwestern Oklahoma. Bull. Am. Assoc. Pet. Geol. 76, 1649–1664.

Gregg, J.M., Sibley, D.F., 1984. Epigenetic dolomitization and the origin of xenotopic dolomite texture. J. Sediment. Petrol. 54, 908–931.

Hanor, J.S., 1987. Origin and migration of subsurface brines: SEPM Lecture Notes #21. Tulsa, OK, 247 pp.

Hovorka, S.D., 1992. Halite pseudomorphs after gypsum in bedded anhydrite—clue to gypsum–anhydrite relationships. J. Sediment. Petrol. 62, 1098–1111.

Kaufman, J., Meyers, W.J., Hanson, G.N., 1990. Burial cementation in the Swan Hills Formation (Devonian), Rosevear Field, Alberta, Canada. J. Sediment. Petrol. 60, 918–933.

Krebs, W., Macqueen, R.W., 1984. Sequence of diagenetic and mineralisation events, Pine Point lead–zinc property, Northwest Territories, Canada. Bull. Can. Pet. Geol. 32, 434–464.

Land, L.S., 1983. The application of stable isotopes to the studies of the origin of dolomites and to problems of diagenesis of clastic sediments. In: Arthur, M.A., Anderson, T.F. (Eds.), Stable Isotopes in Sedimentary Geology. SEPM Short Course, vol. 10, pp. 4.1–4.22.

Land, L.S., Lynch, F.L., 1996. $\delta^{18}O$-values of mudrocks: more evidence for an ^{18}O-buffered ocean. Geochim. Cosmochim. Acta 60, 3347–3352.

Lee, Y.I., Friedman, G.M., 1987. Deep-burial dolomitization in the Ordovician Ellenburger Group carbonates, western Texas and southeastern New Mexico. J. Sediment. Petrol. 57, 544–557.

Lloyd, R.V., Lumsden, D.N., Gregg, J.M., 1985. Relationship between paleotemperatures of metamorphic dolomites and ESR determined Mn(II) partitioning ratios. Geochim. Cosmochim. Acta 49, 2565–2568.

Lumsden, D.N., Lloyd, R.V., 1997. Three dolomites. J. Sediment. Res. 67, 391–396.

Machel, H.-G., 1987. Saddle dolomite as a by-product of chemical compaction and thermochemical sulfate reduction. Geology 15, 936–940.

Machel, H.-G., 2000. Dolomite formation in Caribbean islands—driven by plate tectonics? J. Sediment. Res. 70, 977–984.

Machel, H.-G., Mountjoy, E.W., 1986. Chemistry and environments of dolomitization—a reappraisal. Earth-Sci. Rev. 23, 175–222.

Mathews, R.K., Katz, A., 1977. Oxygen isotope fractionation during dolomitization of calcium carbonate. Geochim. Cosmochim. Acta 41, 1431–1438.

Mazzullo, S.J., 2000. Organogenic dolomitization in peritidal to deep-sea sediments. J. Sediment. Res. 70, 10–23.

McKenzie, J.A., Hsu, K.J., Schneider, J.F., 1980. Movement of subsurface waters under the sabkha, Abu Dhabi, U.A.E. and its relation to evaporative dolomite genesis. In: Zenger, D.H., Dunham, J.B., Ethington, E.L. (Eds.), Concepts and Models of Dolomitization. SEPM Spec. Publ., vol. 28, pp. 11–30.

Meyers, W.J., Lu, F.H., Zachariah, J.K., 1997. Dolomitization by mixed evaporative brines and freshwater, Upper Miocene carbonates, Nijar, Spain. J. Sediment. Res. 67, 898–912.

Montañez, I.P., 1994. Late diagenetic dolomitization of Lower Ordovician, Upper Knox carbonates: a record of the hydrodynamic

evolution of the south Appalachian Basin. Bull. Am. Assoc. Pet. Geol. 78, 1210–1239.

Moss, S., Tucker, M., 1995. Diagenesis of Barremian–Aptian platform carbonates (the Urgonian limestone Formation of SE France): near-surface and shallow-burial diagenesis. Sedimentology 42, 853–874.

Morad, S., Al-asm, I.S., Longstaffe, F.J., Morfil, R., Deros, L.F., 1995. Diagenesis of a mixed siliciclastic/evaporitic sequence of the middle Muschelkalk (Middle Triassic), the Catalan coastal range, NE Spain. Sedimentology 42, 749–768.

Naiman, E.R., Bein, A., Folk, R.L., 1983. Complex polyhedral crystals of limpid dolomite associated with halite, Permian upper Clear Fork and Glorieta Formation, Texas. J. Sediment. Petrol. 53, 549–555.

Peryt, T.M., Scholle, P.A., 1996. Regional setting and role of meteoric water in dolomite formation and diagenesis in an evaporite basin: studies in the Zechstein (Permian) deposits of Poland. Sedimentology 43, 1005–1023.

Radke, B.M., Mathis, R.L., 1980. On the formation and occurrence of saddle dolomite. J. Sediment. Petrol. 50, 1149–1168.

Rodriguez-Navarro, C., Sebastian, E., Rodriguez-Gallego, M., 1997. An urban model for dolomite precipitation: authigenic dolomite on weathered building stones. Sediment. Geol. 109, 1–11.

Sadooni, F.N., 1995. Diagenetic features of some subsurface Tertiary–Cretaceous evaporites from northern Iraq. Carbonates Evaporites 10, 45–53.

Schreiber, B.C., Walker, D., 1992. Halite pseudomorphs after gypsum: a suggested mechanism. J. Sediment. Petrol. 62, 61–70.

Shinn, E.A., Ginsburg, R.N., Lloyd, R.M., 1965. Recent supratidal dolomite from Andros Island, Bahamas. In: Pray, L.C., Murray, R.C. (Eds.), Dolomitization and Limestone Diagenesis. Society of Economic Paleontologists and Mineralogists Spec. Publ., vol. 13, pp. 112–123.

Shukla, V., Baker, P., 1988. Sedimentology and Geochemistry of Dolostones. SEPM Spec. Publ., vol. 43, 266 pp.

Sibley, D.F., Gregg, J.M., 1987. Classification of dolomite rock texture. J. Sediment. Petrol. 57, 967–975.

Smith, T.M., Dorobek, S.L., 1993. Alteration of early-formed dolomite during shallow to deep burial; Mississippian Mission Canyon Formation, central to southwestern Montana. Geol. Soc. Am. 105, 1389–1399.

Sperber, C.M., Wilkinson, B.H., Peacor, D.R., 1984. Rock composition, dolomite stoichiometry and rock/water reactions in dolomitic carbonate rocks. J. Geol. 92, 609–622.

Stanley, S.M., Hardie, L.A., 1999. Hypercalcification: paleontology links plate tectonics and geochemistry to sedimentology. GSA Today 9, 2–7.

Stewart, F.H., 1952. The petrology of the evaporites of the Eskdale no. 2 boring, East Yorkshire. Mineral. Mag. 28, 621–675.

Taylor, R.E., 1937. Water-insoluble residues from the rock-salt of Louisiana salt plugs. Bull. Am. Assoc. Pet. Geol. 21, 1268–1310.

Utha-Aroon, C., 1993. Continental origin of the Maha Sarakham evaporites, northeastern Thailand. J. Southeast Asian Earth Sci. 8, 193–203.

Vahrenkamp, V.C., Swart, P.K., 1994. Late Cenozoic dolomites of the Bahamas: metastable analogues for the genesis of ancient platform dolomite. In: Purser, B., Tucker, M., Zenger, D. (Eds.), Dolomites: A Volume in Honour of Dolomieu. International Association of Sedimentologists, Special Publication, vol. 21, pp. 133–153.

Vasconcelos, C.O., 1994. Modern dolomite precipitation and diagenesis in a coastal mixed water system (Lagoa Vermelha, Brazil): a microbial model for dolomite formation under anoxic conditions [unpublished PhD thesis]: Eidgenossische Technische Hochschule. Zurich, No. 10807, 134 pp.

Vasconcelos, C., McKenzie, J.A., 1997. Microbial mediation of modern dolomite precipitation and diagenesis under anoxic conditions (Lagona Vermelha Rio de Janeiro, Brazil). J. Sediment. Res. 67, 378–390.

Veizer, J., Hoefs, J., 1976. The nature of $^{18}O/^{16}O$ and $^{13}C/^{12}C$ secular trends in sedimentary carbonate rocks. Geochim. Cosmochim. Acta 40, 1387–1395.

Warren, J.K., 1999. Evaporites: Their Evolution and Economics. Blackwell, Oxford, UK, 438 pp.

Weaver, C.E., 1976. Construction of limpid dolomite. Geology 4, 425–428.

Wojcik, K.M., Goldstein, R.H., Walton, A.W., 1994. History of diagenetic fluids in a distant foreland area, Middle and Upper Pennsylvanian, Cherokee Basin, Kansas, USA—fluid inclusion evidence. Geochim. Cosmochim. Acta 58, 1175–1191.

Yoo, C.M., Gregg, J.M., Shelton, K.L., 2000. Dolomitization and dolomite neomorphism: Trenton and Black River Limestones (Middle Ordovician) Northern Indiana, U.S.A. J. Sediment. Res. 70, 265–274.

Zeeh, S., Bechstadt, T., Mackenzie, J., Richter, D.K., 1995. Diagenetic evolution of the Carnian Wetterstein platforms of Eastern Alps. Sedimentology 42, 199–222.